Department of Geosciences
The Pennsylvania State University
University Park, PA 16802

Final Report for June 15, 1996 to June 15, 2000
to the

U. S. Department of Energy
Geosciences Research Program
Office of Basic Energy Sciences

On

Grant No. DE-FG02-96ER14634

ZEOLITE THERMODYNAMICS AND KINETICS

H. l. Barnes, R. T. Wilkin, and L. G. Benning

June 15, 2000

DISCLAIMER

This final report summarizes results obtained under this project on the thermodynamic and kinetic properties of zeolites. Zeolites, common in a variety of geological environments, are abundant in volcanics, including tuffaceous sediments and vugs and veins, especially of basalts where they may affect primary fracture permeability (e.g., Coombs et al., 1959; Hay, 1966; Iijama and Utada, 1966; Sheppard and Gude, 1969; Kastner and Stonecipher, 1978; Kristamnndottir and Tomasson, 1978; Gottardi and Galli, 1985). Although clearly important to understanding the distribution of zeolites (e.g., Liou, 1970, 1971; Boles, 1972; Abe and Aoki, 1976; Dibble and Tiller, 1981; McCulloh et al., 1981; Barrer, 1982; Zeng and Liou, 1982; Bish, 1984; Hemingway and Robie, 1984; Johnson et al., 1983, 1985, 1991, 1992; Cho et al., 1987; Howell et al., 1990; Bish, 1990; Feng and Savin, 1993; Pabalan, 1994; Murphy et al., 1996), thermodynamic and kinetic characteristics of zeolites have been only partially evaluated. Major questions persist on the processes of zeolite formation and diagenesis. These include the pressure-temperature-dependence of zeolite stabilities and reaction rate-dependence on alkali cation and Al/Si contents, and the hydration state (e.g., Kiselva et al., 1996a,b; Carey and Bish, 1996; Petrovic and Navrotsky, 1997). Together, closed-system and flow-through-system hydrothermal techniques, which were adapted for experimental investigations of the zeolites, systems have recently provided important progress on these problems (e.g., Wilkin and Barnes, 1998b).

Funding of this research on the "Thermodynamics and Kinetics of Zeolites" supported the development of techniques of material preparation as well as experimental strategies and methods for measuring solubilities, hydration states, and rates of zeolite dissolution, precipitation, and nucleation. Our hydrothermal experiments have provided temperature-dependent solubility products, hydration states, and a set of standard free energies of formation for end-member Na-, K-, and Ca-clinoptilolite, mordenite, and analcime (Wilkin and Barnes, 1998b; Wilkin and Barnes, 1999; Benning, Wilkin, and Barnes, 2000). In addition, flow-through experimental methods have been used to measure the rates of Na-clinoptilolite and analcime dissolution and precipitation as a function of reaction affinity to 250°C, and, most recently, the experimental system has been modified so that the clinoptilolite-to-analcime transformation was monitored and its rates and mechanisms evaluated (Wilkin and Barnes, 1996; 1998b). This research has direct applications to repository behavior, diagenesis, and low-grade metamorphism. Furthermore, the experimental data characterize environments where zeolites are used as sorptive barriers to migration of contaminants, and for industrial applications in which zeolites are used as catalysts, cation exchangers and molecular sieves. In each of these applications, there has been a serious need for quantitative data on the kinetic and thermodynamic stabilities of zeolites.

Research Objectives

The original goals of this project were to evaluate both the thermodynamics and kinetics of zeolite-water reactions to about 300°C. Research plans originally emphasized analcime, clinoptilolite, and mordenite because of their natural abundances, particularly in the volcanic rocks in, and near, Yucca Mountain, Nevada. Solubility measurements are direct and accurate means of deriving thermodynamic data for alumino-silicates,

useful for evaluation of steady-state concentrations of solutions co-existing with zeolites, but also to evaluate mass transfer processes. Our work has demonstrated that the derivation of accurate thermodynamic properties from the solubility products of zeolites also requires knowing the state of zeolite hydration. It is normally assumed that the amount of zeolite-water at all temperatures is equal to that measured at room temperature, based on weight loss after ignition or from conventional thermogravimetric analyses. Consequently, an important extension of the originally proposed research was to determine the hydration state of clinoptilolite to 300°C and as a function of the thermodynamic activity of water. An early key conclusion from this work is that high quality thermodynamic data for hydrated zeolites, such as clinoptilolite, whether obtained by calorimetry or solubility methods, must be based on measurements that define what has been the poorly known state of zeolite hydration.

Kinetic data on dissolution and growth rates were to be obtained from flow-through hydrothermal experiments. In such experiments the rate, R, of accumulation of some aqueous species, i, over time at temperature, T, and pressure, P, can be described by

$$R_i = (\partial n_i/\partial t)_{T,\,P,\,M,\,\omega} \tag{1}$$

where n_i is the number of moles of species i, M is the mass of solution, and ω is the mass flow rate through the reactor. The net rate of reaction of species i can be defined as

$$R_{i,\,rxn} = 1/A n_i(\partial n_i/\partial t)_{T,P,A,M} \tag{2}$$

Thus, if the supply and removal of aqueous reactants and products are constant with time, and the stoichiometry of reactions (ν), surface area (A), and mass of solution in the reactor are time-independent, the apparent rate of reaction is reduced to a function of T, P, and the physicochemical properties of the solid. In a well-mixed, flow-through reactor the rate of, for example, dissolution may be obtained when input and output concentrations (C) are at steady state by the equation

$$R = \omega/\nu A(C_{i,out}-C_{i,in}) \tag{3}$$

Finally the degree of saturation with respect to the phase investigated can be determined by the familiar equation

$$\Delta G = RT\ln(IAP/K_{sp}) \tag{4}$$

where R is the gas constant, T is absolute temperature, IAP is the ion activity product, and K_{sp} is the solubility of the mineral obtained in the closed-system experiments as described above.

An important goal of our research was to expand the kinetic treatment described above for mineral dissolution and growth processes to the kinetics of the clinoptilolite-to-analcime reaction. The coupled processes of clinoptilolite dissolution and analcime nucleation and growth are characteristic of diagenesis and low-grade metamorphism of

sedimentary and volcanic rocks. Confusion about the rate and mechanism of this mineral reaction causes intractable problems for modeling the long-term behavior of the Yucca Mountain repository. Consequently, our research efforts were to be especially concentrated on the clinoptilolite-to-analcime reaction. Our approach of investigating this reaction by simultaneously examining solid and solution compositions allows resolution *separately* of both analcime nucleation and growth, processes rarely evaluated individually. We believe that this technique could serve as a general guide for future research on the mineral transformation kinetics of reactions, both among zeolites and for other silicates.

Results under this DOE Project

This section summarizes results obtained primarily during the past 4 years during our investigation of the thermodynamics and kinetics of zeolites. Significant project milestones include three publications: *Solubility and stability of zeolites in aqueous solution. I: analcime, Na-, and K-clinoptilolite*, (Am. Min., 1998b); *Thermodynamics of hydration of Na- and K-clinoptilolite to 300°C*, (Phys. Chem. Min., 1999); and *Solubility and stability of zeolites in aqueous solution. II: calcic clinoptilolite and mordenite* (Am. Min., 2000). In addition, a paper is in press on kinetic aspects of this research (Aam. Min., 2000), *Nucleation and growth of analcime from precursor Na-clinoptilolite* where the rates for nucleation and for crystal growth are each have been evaluated. Each of these contributions includes a large quantity of new experimental data. A total of seven, often invited, oral papers have also been presented at professional meetings.

Following is a summary of our current understanding of zeolites on zeolite solubilities, hydration thermodynamics, and reaction kinetics achieved under this past D.O.E. grant.

1. Zeolite Solubilities

The solubilities of analcime, clinoptilolite, and mordenite were determined in dilute, weakly alkaline, aqueous solutions up to 300°C and at vapor-saturated pressures (Wilkin and Barnes, 1998b; Benning, Wilkin, and Barnes, 2000). Experimental methodologies are described in Appendix A. Prepared samples for the experiments were analcimes from Mont St. Hilaire, Quebec (an_1: Si/Al = 2.02) and Wikieup, Arizona (an_2: Si/Al = 2.55), clinoptilolite samples were from Castle Creek, Idaho (Si/A l= 4.50), and mordenite samples were from Poona, India (Si/Al = 4.98). The effects of alkali content (Na, K, Ca) on clinoptilolite and mordenite solubility were determined by using cation-exchanged varieties of the Castle Creek and Poona materials. In neutral to weakly alkaline solutions, the dominant solubility-controlling reactions of, for example, the Mont St. Hilaire analcime is:

$$NaAlSi_2O_6{\cdot}H_2O(an_1) + 5H_2O(l) \Leftrightarrow Na^+ + Al(OH)_4^- + 2Si(OH)_4(aq) \qquad (5)$$

The experimental data provide values for log K as shown in Figure 1. The best fit between the data where the points were approached from undersaturation and those from supersaturation are given as the logarithm of the equilibrium constants of these reactions and are fit to the function:

$$\log K = A + BT + C/T + D \log T.$$

The regression coefficients are summarized in Table 1. At 25°C, log K_{25} values for the Mont St. Hilaire analcime, Wikieup analcime, Na-clinoptilolite, K-clinoptilolite, and Ca-

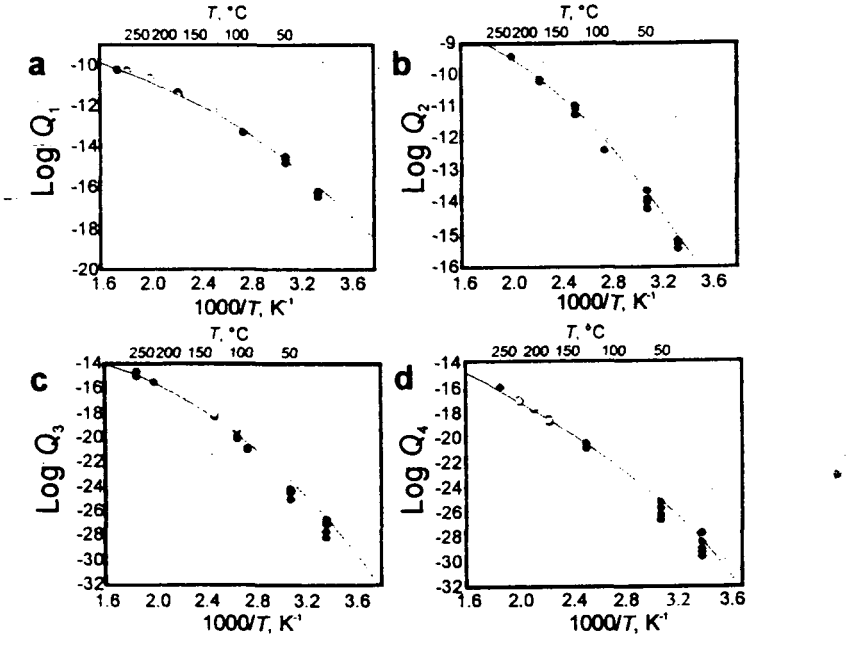

Figure 1. Log K vs. 1000/T plots for (a) Mont St. Hilaire analcime; (b) Wikieup analcime; (c) Castle Creek Na-clinoptilolite; and (d) Castle Creek K-clinoptilolite. Filled circles indicate sampling conditions approached from undersaturation and open circles indicate sampling approached from supersaturation.

clinoptilolite are –16.1, -15.0, -26.5, and –28.1, -26.8 respectively. These data were combined with the thermodynamic properties of the aqueous species $Si(OH)_4$, $Al(OH)_4^-$, Na^+, K^+, Ca^{2+}, and liquid water to determine standard Gibbs free energies of formation as a function of temperature.

Values of $\Delta G°_f$ at 25°C and 1 bar for the Mont St. Hilaire analcime and Wikieup analcime are –3089.2 ± 5 and –3044.4 ± 5 kJ/mol, respectively. The $\Delta G°_f$ values for fully hydrous Na-clinoptilolite, K- clinoptilolite, and Ca-clinoptilolite, respectively, are –6267.9 ± 10, –6107.4 ± 10, and –6386.0 ± 10 kJ/mol at 25°C and 1 bar. The solubility data reported here, and results obtained from previous calorimetric studies, indicate that the aluminosilicate frameworks of analcime and clinoptilolite are stabilized by an increase in Al content.

TABLE 1. Temperature dependence of zeolite solubility products.

Mineral	A	B	C	D
Analcime (Si/Al=2.0) Mont St. Hilaire	224.898	0.026	- 13609.700	-82.060
Analcime (Si/Al=2.5) Wikieup	224.489	0.029	- 13420.200	-82.105
Na-clinoptilolite (Si/Al=4.5)	745.150	0.100	- 38200.428	-272.100
K-clinoptilolite (Si/Al=4.5)	741.850	0.103	- 37980.452	-272.088
Ca-clinoptilolite (Si/Al=4.4)	-170.214	-0.025	-5.624	60.988
Na-mordenite	750.15	0.100	-38500.3	-271.9
K-mordenite	748.23	0.101	-38800.2	-271.5
Ca-mordenite (Si/Al=4.8)	-348.22	-0.107	-170.581	142.023

Note: $\log K = A + BT + C/T + D \log T$, where T is in kelvins. Data presented in Wilkin and Barnes (1998b) and Benning, Wilkin, and Barnes (2000)

Zeolite solubility data make possible the evaluation of reactions among zeolites, for example, the clinoptilolite-to-analcime reaction. Analysis of the temperature-dependent log K values indicates that analcime formation is favored when aqueous silica concentrations are equal to quartz saturation. In solutions saturated with cristobalite, analcime formation is favored above 50°C. The persistence of clinoptilolite to temperatures near 175°C in some hydrothermal environments suggests that kinetic factors, rather than equilibrium silica concentrations, control this replacement process.

The methods of material preparation and solubility measurements developed and described in Wilkin and Barnes (1998b) serve as guide for solubility studies on other zeolites. The solubility data are useful sources of thermodynamic data, but perhaps more importantly, as described below, the data provide necessary information for designing kinetic experiments.

2. Thermodynamics and Kinetics of Clinoptilolite Hydration

Three intensive parameters, water vapor pressure (P_{H_2O}), temperature, and water adsorption capacity define the clinoptilolite-water system. Boles (1972) discovered that the amount of water in natural specimens of clinoptilolite correlates with cation content. Clinoptilolites enriched in divalent cations generally contain more water than clinoptilolites enriched in Na and K. Thus, for any fixed cation composition of clinoptilolite, the amount of clinoptilolite-water is a function of P_{H_2O} and T. A model to compute the amount of zeolitic-water, at any P and T, is crucial in thermochemical

calculations involving these hydrated minerals (e.g., Carey and Bish, 1996) because of the large ΔG of hydration involved.

The derivation of accurate thermodynamic properties from solubility products also requires knowing the state of clinoptilolite hydration. For example, idealized dissolution of Na-clinoptilolite follows

$$NaAlSi_5O_{12}\cdot 4H_2O + 8H_2O \Rightarrow Na^+ + Al(OH)_4^- + 5Si(OH)_4 \quad (6)$$

If the standard state of unit activity is taken to be the pure minerals and fluids at the temperature and pressure of interest, the logarithm of the solubility product can be computed with

$$\log K_{sp} = \log a_{Na+} + \log a_{Al(OH)4-} + 5\log a_{Si(OH)4} \quad (7)$$

and the standard Gibbs free energy of formation, ΔG_f°, of Na-clinoptilolite (Na-cpt) can be calculated from

$$\Delta G_f^\circ{}_{Na\text{-}cpt} = 8\Delta G_f^\circ{}_{H2O} - \Delta G_f^\circ{}_{Na+} - \Delta G_f^\circ{}_{Al(OH)4-} - 5\Delta G_f^\circ{}_{Si(OH)4} - (2.303RT\log K_{sp}) \quad (8)$$

It is normally assumed that the water content of clinoptilolite at all temperatures is equal to that measured at room temperature, based on weight loss after ignition. However, if at elevated temperatures and saturated vapor pressures the amount of clinoptilolite-water changes, as for example decreasing by one half, than the mass balance of reaction (6) requires that 10 instead of 8 moles of H_2O must react to dissolve 1 mole of Na-cpt. The Gibbs free energy of formation would then decrease by about 520 kJ/mol (at 250°C) or about 8% of the total free energy of the mineral. The important conclusion is that accurate thermodynamic data for hydrated zeolites such as clinoptilolite, whether obtained either by calorimetry or solubility methods, requires measurements to define the typically poorly known state of zeolite hydration under most conditions.

Consequently, we designed and constructed a system (see Appendix A) to measure the hydration state of zeolites as a function of temperature and P_{H2O}. By this pressure titration method, the hydration states of Na- and K-exchanged clinoptilolites (Castle Creek, Idaho) have been measured to 300°C and $P_{H2O} < 30$ bars (Wilkin and Barnes, 1999). Equilibrium constants are determined from hydration isotherms. The equilibrium constants were modeled with a sub-regular mixing model, and thus provide a standard set of thermodynamic parameters for the hydration reaction. The water content of clinoptilolite can be predicted as a function of activity (or pressure) and temperature with the equation:

$$a_{H2O} = [\exp[[-\Delta H_h^\circ/nRT] + [\Delta S_h^\circ/nR] - 1/nRT\cdot[W_1X_h + W_2X_h^2] - \ln(X_a/X_h)]]^{-1} \quad (9)$$

where T is degrees in Kelvin, ΔH_h° is the standard-molal enthalpy of hydration, ΔS_h° is the entropy of hydration, X_h and X_a are, respectively, the mole fractions of the hydrous and anhydrous components of the solid solution, W_1 and W_2 are interaction parameters, n

is the maximum number of moles of H_2O per mineral formula unit (based on 12 oxygens), and R is the gas constant. For convenience, the state of maximum hydration is taken to be the hydration state at 25° and 50% relative humidity. This equation can be used to locate clinoptilolite-H_2O isohydrons in a_{H2O}-T space below the liquid-vapor equilibrium curve of water. To use this equation, a value of the hydration coefficient, x, is selected based on 12 oxygens per clinoptilolite formula unit such that $x < n$, thus, fixing X_h and X_a. For example selecting x=1.5 for sodium clinoptilolite gives X_h=1.5/3.48=0.431 and X_a=1-X_h=0.569, fixing the isohydron for x=1.5 in a_{H2O}-T space.

In Figure 2 are shown several isohydrons for Na-clinoptilolite calculated using the standard-state thermodynamic values listed in Table 2 and Equation (9). The 1σ confidence interval of the x=1.5 isohydron is indicated in Figure 2 by the shaded area around the contour. The uncertainty in the a_{H2O}-T positions of the isohydrons is estimated using the standard error of the Gibbs free energy of hydration and enthalpy of hydration (Table 2).

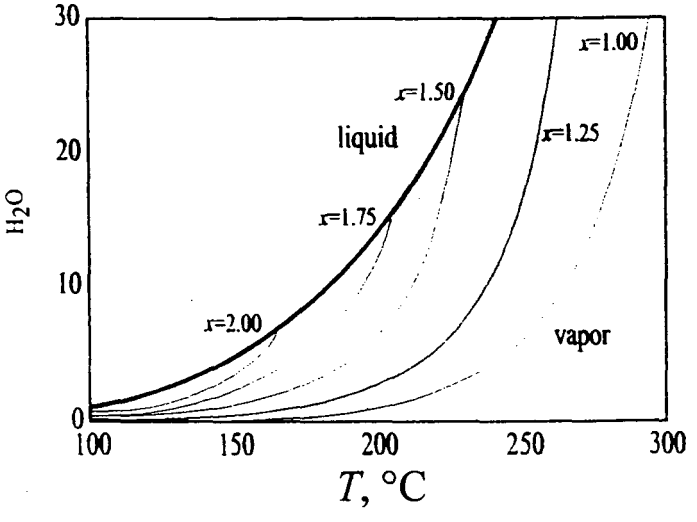

Figure 2. Contours of constant H_2O content (isohydrons) in Na-clinoptilolite where x is the number of moles of water per mole of anhydrous clinoptilolite.

TABLE 2. Standard molal thermodynamic properties of clinoptilolite hydration at 25 °C and 1 bar

	$\Delta G_h°$	$\Delta H_h°$	$\Delta S_h°$	W_1	W_2
Na-cpt	-165,707	-367,244	-676.0 ±	227,122	-124,411
	± 19.2	± 19.5	25.1	± 23,436	± 12,207
K-cpt	-120,337	-269,055	-498.9 ±	167,554	-88,194
	± 7.2	± 13.8	9.5	± 8,951	± 3,120

Notes: Units are kJ/mol for $\Delta G_h°$ and $\Delta H_h°$, J/mol·K for $\Delta S_h°$, and J/mol for W_1 and W_2. Standard errors were determined from regression analysis and represent the 1 σ confidence level. Thermodynamic properties per mole of H_2O in clinoptilolite may be obtained by dividing the values in the table by n, 3.48 or 2.65, for Na- and K-clinoptilolite, respectively

The standard molal Gibbs free energy of hydration is –47.62 ± 5.52 kJ/mol H_2O and –45.41 ± 2.71 kJ/mol H_2O for Na- and K-clinoptilolite, respectively. These standard-state thermodynamic properties of clinoptilolite hydration are in good agreement with published data for very low H_2O pressures (Carey and Bish, 1996). The pressure-titration experiments indicate that clinoptilolite progressively dehydrates with increasing temperature and pressures along the liquid-vapor equilibrium curve for water. Our kinetic data show that clinoptilolite dehydration and hydration processes are fast and reversible and that steady-state hydration states are attained in minutes.

3. Kinetics of Zeolite Reactions

Equilibrium stability fields among Na-clinoptilolite, analcime, kaolinite, and boehmite at 175 °C are shown by the phase boundaries in Figure 3. Note that in the construction of this diagram, mineral stabilities are based on the solubility data that were described in Part 1 of this section. Thus far, most of the flow-through experiments at 175 °C have been carried out in solutions with $\Sigma(Na)=0.01m$ and pH=8 where $Al(OH)_4^-$ and $Si(OH)_4$ are the dominant aqueous Al and Si species, respectively. Also shown in Figure 3 are the compositions of outflowing solutions in the seeded, dissolution or precipitation runs for reactions from Na-clinoptilolite (marked A_2, blue box) and from analcime (marked A_1, red box). Note that for the Na-clinoptilolite dissolution experiments, outflowing solutions fall well into the stability fields of analcime and kaolinite, and for analcime dissolution experiments, outflowing solutions fall in the stability fields of kaolinite and boehmite. Because in these experiments at pH 8 phase transformations were not observed, concluded is that homogeneous or heterogeneous nucleation of the thermodynamically stable phases does not occur for the most stable phases close to the stability field boundaries of clinoptilolite or analcime. Alternatively, the nucleation kinetics of these other, stable phases were sufficiently slow such that detectable quantities did not accumulate over the duration of the experiments (~1-3 weeks) or alter the measured congruent release of Al and Si.

The kinetics of dissolution and precipitation of analcime and Na-clinoptilolite in hydrothermal solutions were presented orally at the *V. M. Goldschmidt Conference* in Tucson (Wilkin and Barnes, 1997). The overall analcime dissolution reaction in solutions where $Al(OH)_4^-$ and $Si(OH)_4$ species are dominant (pH ~8) is best expressed as:

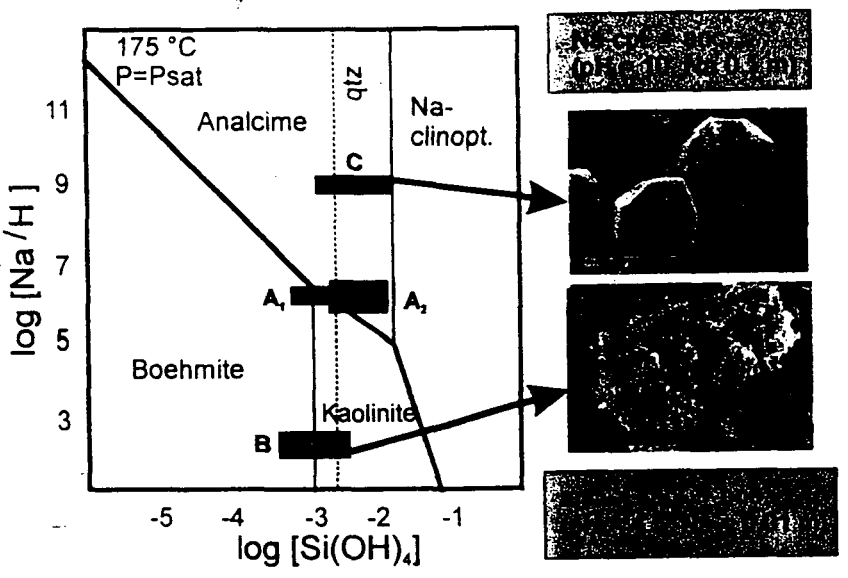

Figure 3. Phase relations at 175°C (see text for descriptions of regions A-C).

$$NaAlSi_2O_6{\cdot}H_2O + 5H_2O \Rightarrow Na^+ + Al(OH)_4^- + 2Si(OH)_4 \qquad (10)$$

Dissolution rates can be described by:

$$\text{Rate} = -k_1{*}(1-e^{\Delta Gr/RT})^2 \qquad (11)$$

where the dissolution rate is expressed in (mol m^{-2} sec^{-1}); the gas constant, R; and T, temperature, in K. The rate constant, k_1 (mol m^{-2} sec^{-1}), is $4.1x10^{-10}$, $2.0x10^{-9}$, $4.2x10^{-9}$, and $6.3x10^{-9}$ at 125°, 175°, 225°, and 250°C, respectively. Precipitation rates were measured at 125° and 175°C and linearly depend on ΔG_r as in

$$\text{Rate} = k_2{*}(\Delta G_r/RT) \qquad (12)$$

where k_2 is equal to $0.56x10^{-10}$ and $1.89x10^{-10}$ at 125° and 175°C, respectively. Based on the rate constants for analcime dissolution (reaction 10), the Arrhenius model gives an E_a of 8.89 ± 1.5 kcal mol^{-1}. An identical E_a (8.8 kcal mol^{-1}) is obtained for the analcime precipitation reaction based on measurements at 125° and 175°C.

Having achieved stoichiometric dissolution behavior in slightly alkaline solutions, the next approach was to measure analcime dissolution rates in slightly acidic solutions (pH=4.5) where $Si(OH)_4$ and $Al(OH)_3$, (instead of $Al(OH)_4^-$), are the dominant Si and Al species, respectively. The overall dissolution reaction in such mid-pH solutions should follow

$$NaAlSi_2O_6{\cdot}H_2O + 4H_2O + H^+ \Rightarrow Na^+ + Al(OH)_3 + 2Si(OH)_4 \qquad (13)$$

The low-pH experiments, however, were at first considered to be failures because stoichiometric release of Al and Si was not observed and, upon X-ray diffraction and SEM analyses, found were a mixture of fine-grained boehmite and kaolinite that coated the surfaces of the initial analcime seed materials (Fig. 3). After a 1 week period at 175°C, the solids consisted of both an ~20 wt% mix of boehmite and kaolinite and ~80 wt% analcime. The outflowing solutions fall in box B on Figure 3. Note that box B is far from the analcime stability field so that sufficient overstepping overcame the kinetic nucleation barriers of boehmite and kaolinite.

The results indicate that, at pH 4.5, reaction (13) is rate-limiting to the precipitation of kaolinite and boehmite, and that analcime will not persist in even slightly acidic solutions. More importantly, dissolution and precipitation studies of zeolites and other aluminosilicates (including feldspars) are likely to be congruent only where $Al(OH)_4^-$ is the dominant Al species in solution. The results also suggest that the so-called pH effect on reaction rates may be very difficult to evaluate except across narrow, alkaline pH segments.

Examination of Figure 3 indicates that the Na-clinoptilolite-to-analcime conversion should be driven by decreasing the activity of $Si(OH)_4$, especially in solutions with high Na^+/H^+. To test this hypothesis, a high pH (9.7) experiment was set up (Region C on Fig. 3). This required changing over from the normal, Ti-17 alloy reaction and feeder vessels to those composed of base-resistant stainless steel (SS316 or SS310). In an initial experiment at 200°C, the conversion was quick, – 100% complete in <24 hours. The analcime produced was remarkably well-crystallized, having cubic trapezohedral forms typical of sedimentary analcime (Fig. 3). The particles ranged in size from 3 to 15 μm.

Subsequent experiments explored the clinoptilolite to analcime reaction at 125-225°C, ΣNa^+=0.1 *m*, and pH=9.8. The experimental flow-through design allows for the sampling of both solutions and solids through time. In Figure 4 are data that were collected with this system and are used to resolve separately both nucleation and growth rates. In an open, flow-through system where clinoptilolite reacts to form analcime, mass is continually lost from the reaction system; i.e., there is an excess of clinoptilolite dissolution over analcime precipitation. Time-resolved X-ray diffraction data and measured solution compositions are suitable bases for determining both the absolute losses and gains in the mass of clinoptilolite and analcime, respectively. The increase in analcime mass depends upon both nucleation and growth processes. Initially, analcime particles are very fine-grained (<5 μm) and have spheroidal morphology. However, with continued reaction, the size distribution broadens, particle morphology becomes euhedral, and the mean particle size increases (Fig. 4). The change in the number of analcime particles in the system with time is determined from the size distribution and X-ray data. The rate of change of the number of analcime particles is a precise measure of the rate of analcime nucleation. Average growth rates are obtained by considering the change with time of the median and maximum particle sizes (Wilkin and Barnes, 1998b).

The overall goals of this research are to quantify the rate of analcime *nucleation* as a function of temperature and saturation state, and to compare this nucleation function

with *T*- and saturation-state-dependent analcime *growth rates* obtained from seeded, flow-through experiments. We are not aware of any other study where both *nucleation* and *growth* kinetics are independently evaluated. Consequently, we believe that this research should lead to fundamental improvements in our understanding of reaction mechanisms involving zeolites while at the same time yielding data required for modeling long-term repository behavior.

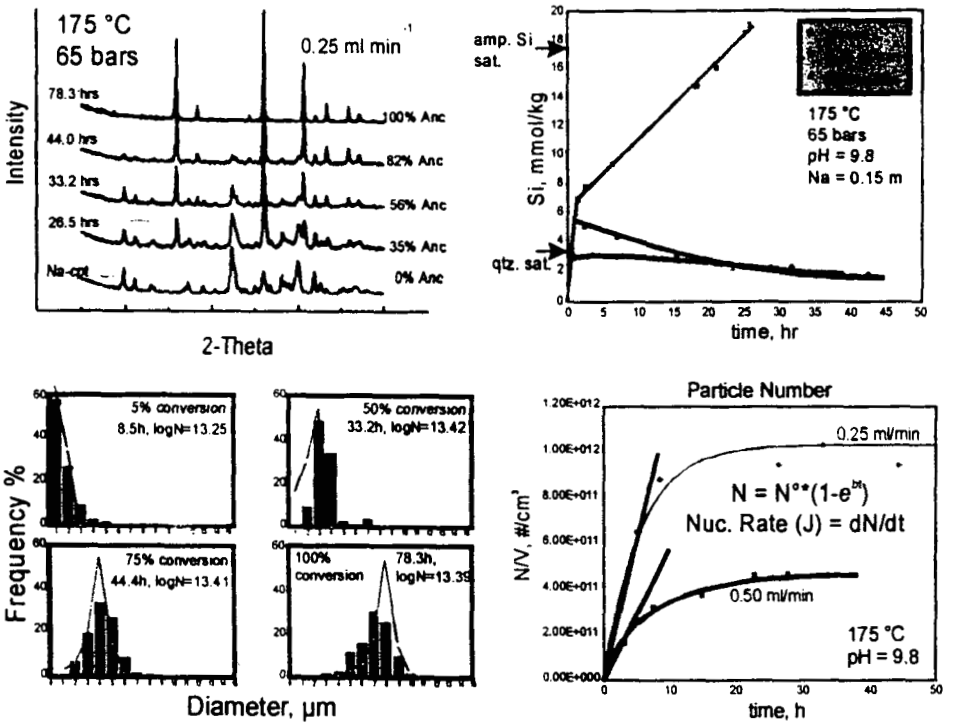

Figure 4. Change of X-ray, solution, and particle crystallization data.

CONCLUSIONS

Solubility measurements are a comparatively direct and accurate means of deriving thermodynamic data for aluminosilicate minerals, primarily because of the precise database available on Al and Si speciation in aqueous solutions to 350°C (e.g., Bourcier et al., 1993). Measurements of zeolite solubilities in aqueous solutions ensure that a constant state of hydration can be maintained. Furthermore, the cation compositions can be controlled by proportional cation exchange prior to solubility measurements. By these methods, relatively precise solubility products and derived thermodynamic constants can be determined for zeolites with Na-, K-, and Ca-endmember and intermediate compositions. The derivation of accurate thermodynamic properties of zeolites from solubility products also requires knowing exactly the state of zeolite hydration. During the grant period, we have developed a pressure-titration method to measure the hydration state of hydrous materials to 300°C and at water vapor

pressures up to the liquid-vapor curve. A complete thermodynamic model of zeolites can then be obtained by combining the results of solubility and hydration experiments.

The above thermodynamic data provide a basis for correlating measurements of dissolution and precipitation reaction rates with measured or specified departures from equilibrium conditions. The use of flow-through experimental equipment represents the state-of-the-art in geochemical kinetics research techniques because reaction rates can be tracked under conditions of fixed fluid composition, flow rate, temperature, and pressure. Under this grant, the flow-through methodology was used to evaluate the kinetics of dissolution and growth processes, especially for clinoptilolite and analcime. The experiments demonstrate that congruent dissolution behavior is only observed in a narrow, alkaline pH range. At acidic and alkaline conditions, zeolites rapidly react at temperatures >100°C to form more stable phase assemblages. The flow-through methodology was extended to examine the kinetics of the clinoptilolite to analcime reaction. This was done in alkaline solutions by simultaneously examining compositions of solids and solution continuously to permit the separate resolution of rates of analcime nucleation and growth. We believe that these new methodologies of experimentation and data analysis will serve as templates for future research on mineral transformation kinetics.

ORAL AND WRITTEN PAPERS RESULTING FROM THIS SUPPORT

Benning, L., Wilkin, R. and Barnes, H., 1997. The solubility of Ca- and Mg-clinoptilolite, Seventh Annual V.M. Goldschmidt Conference, Tucson, AZ, pp. 25.

Benning, L., Wilkin, R. and Barnes, H.L., 2000. Solubility and stability of zeolites in aqueous solution. II: Calcic clinoptilolite and mordenite. American Mineralogist, 85: 495-508.

Wilkin, R.T. and Barnes, H.L., 1996. Solubilities of Na- and K-clinoptilolite in hydrothermal solutions, Journal of Conference Abstracts, v. 1, Sixth Annual V. M. Goldschmidt Conference, Heidelberg, pp. 672.

Wilkin, R.T. and Barnes, H.L., 1996. Analcime dissolution and precipitation kinetics at 175°C and pH 8, Geological Society of America Annual Meeting, Denver, CO, pp. A33.

Wilkin, R.T. and Barnes, H.L., 1997. Temperature and free energy dependence of zeolite precipitation and dissolution rates, Seventh Annual V. M. Goldschmidt Conference. Lunar and Planetary Institute, Houston, Tucson, AZ, pp. 219.

Wilkin, R.T. and Barnes, H.L., 1998a. Kinetics of the clinoptilolite to analcime reaction, Geological Society of America Annual Meeting, Toronto, ON, pp. A188.

Wilkin, R.T. and Barnes, H.L., 1998b. Solubility and stability of zeolites in aqueous solution. I: Analcime, Na-, and K-clinoptilolite. American Mineralogist, 83: 746-761.

Wilkin, R.T. and Barnes, H.L., 1999. Thermodynamics of hydration of Na- and K-clinoptilolite to 300°C. Physics and Chemistry of Minerals, 26: 468-476.

Wilkin, R. and Barnes, H., 2000, Nucleation and growth kinetics of analcime from precursor Na-clinoptilolite. American Mineralogist, 85: in press.

Wilkin, R.T., Benning, L.G. and Barnes, H.L., 1996. Processes of zeolite formation and transformation from diagenesis to greenschist facies: Constraints from hydrothermal solubility and kinetic experiments, Research Conference on Geochemistry of Crustal Fluids, Seefeld, Austria, pp. 93.

Wilkin, R.T., Benning, L.G. and Barnes, H.L., 1997. Measurement of zeolite hydration states, Proceedings of the Fifth International Symposium on Hydrothermal Reactions, Gatlinburg, TN, pp. 88-91.

BIBLIOGRAPHY

Abe, H. and Aoki, M., 1976. Experiments on the interaction between Na_2CO_3-$NaHCO_3$ solution and clinoptilolite tuff, with reference to analcimization around Kuroko-type mineral deposits. Chemical Geology, 17: 89-100.

Barnes, H.L., 1971. Investigations in hydrothermal sulfide systems. In: G.C. Ulmer (Editor), Research Techniques for High Pressure and Temperature. Springer-Verlag, New York, pp. 317-355.

Barrer, R.M., 1982. Hydrothermal chemistry of zeolites. Academic Press, New York.

Bish, D.L., 1984. Effects of exchangeable cation composition on the thermal expansion/contraction of clinoptilolite. Clays and Clay Minerals, 32: 444-452.

Bish, D.L., 1990. Long-term thermal stability of clinoptilolite: the development of a "B" phase. European Journal of Mineralogy, 2: 771-777.

Boles, J.R., 1972. Composition, optical properties, cell dimensions, and thermal stability of some heulandite group zeolites. American Mineralogist, 57: 1463-1493.

Bourcier, W.L. and Barnes, H.L., 1987. Rocking autoclaves for hydrothermal experiments I. fixed volume systems. In: G.C. Ulmer and H.L. Barnes (Editors), Hydrothermal Experimental Techniques. John Wiley & Sons, New York, pp. 189-215.

Bourcier, W.L., Knauss, K.G. and Jackson, K.J., 1993. Aluminum hydrolysis constants to 250 °C from boehmite solubility experiments. Geochimica et Cosmochimica Acta, 57: 747-762.

Carey, J.W. and Bish, D.L., 1996. Equilibrium in the clinoptilolite-H_2O system. American Mineralogist, 81: 952-962.

Cho, M., Maruyama, S. and Liou, J.G., 1987. An experimental investigation of heulandite-laumontite equilibrium at 1000 to 2000 bar P_{fluid}. Contributions to Mineralogy and Petrology, 97: 43-50.

Coombs, D.S., Ellis, A.J., Fyfe, W.S. and Taylor, A.M., 1959. The zeolite facies, with comments on the interpretation of hydrothermal syntheses. Geochimica et Cosmochimica Acta, 17: 53-107.

Crerar, D.A. and Barnes, H.L., 1976. Ore solution chemistry V. Solubilities of chalcopyrite and chalcocite assemblages in hydrothermal solutions at 200° to 350°C. Economic Geology, 71: 772-794.

Dibble, W.E. and Tiller, W.A., 1981. Kinetic model of zeolite paragenesis in tuffaceous sediments. Clay and Clay Minerals, 29: 323-330.

Feng, X. and Savin, S.M., 1993. Oxygen isotope studies of zeolites-stilbite, analcime, heulandite, and clinoptilolite II. kinetics and mechanisms of isotopic exchange. Geochimica et Cosmochimica Acta, 57: 4219-4238.

Giordano, T.H. and L., B.H., 1979. Ore solution chemistry VI. PbS solubility in bisulfide solutions to 300°C. Economic Geology, 74: 1637-1646.

Gottardi, G. and Galli, D., 1985. Natural Zeolites. Springer-Verlag, Berlin, 409 pp.

Hay, R.L., 1966. Zeolites and zeolitic reactions in sedimentary rocks, 85. Geological Society of America Special Paper, 130 pp.

Helgeson, H.C. and Kirkham, D.H., 1974. Theoretical prediction of the thermodynamic behavior of aqueous electrolytes at high pressures and temperatures: II. Debye-Huckel parameters for activity coefficients and relative partial-molal properties. American Journal of Science, 274: 1199-1261.

Hemingway, B.S. and Robie, R.A., 1984. Thermodynamic properties of zeolites: low temperature heat capacities and thermodynamic functions of phillipsite and clinoptilolite. Estimates of the thermochemical properties of zeolitic water at low temperatures. American Mineralogist, 69: 692-700.

Howell, D.A., Johnson, G.K., Tasker, I.R., O'Hare, P.A.G. and Wise, W.S., 1990. Thermodynamic properties of the zeolite stilbite. Zeolites, 10: 525-531.

Iijima, A. and Utada, M., 1966. Zeolites in sedimentary rocks, with reference to the depositional environments and zonal distribution. Sedimentology, 7: 327-357.

Johnson, G.K., Flotow, H.E. and O'Hare, P.A.G., 1983. Thermodynaic studies of zeolites: natrolite, mesolite, scolecite. American Mineralogist, 68: 1134-1145.

Johnson, G.K., Flotow, H.E. and O'Hare, P.A.G., 1985. Thermodynamic studies of zeolites: heulandite. American Mineralogist, 70: 1065-1071.

Johnson, G.K., Flotow, H.E., O'Hare, P.A.G. and Wise, W.S., 1982. Thermodynamic studies of zeolites: analcime and dehydrated analcime. American Mineralogist, 67: 736-748.

Johnson, G.K., Tasker, I.R., Flotow, H.E., O'Hare, P.A.G. and Wise, W.G., 1992. Thermodynamic studies of mordenite, dehydrated mordenite, and gibbsite. American Mineralogist, 77: 85-93.

Johnson, G.K., Tasker, I.R., Jurgens, R. and O'Hare, P.A.G., 1991. Thermodynamic studies of zeolites: clinoptilolite. Journal of Chemical Thermodynamics, 23: 475-484.

Kastner, M. and Stonecipher, S.A., 1978. Zeolites in pelagic sediments of the Atlantic, Pacific, and Indian Oceans. In: L.B. Sand and F.F. Mumpton (Editors), Natural zeolites: occurrence, properties , use. Pergamon Press, New York, pp. 199-220.

Kiselva, I., Navrotsky, A., Belitsky, I.A. and Fursenko, B.A., 1996a. Thermochemistry and phase equilibria in calcium zeolites. American Mineralogist, 81: 658-667.

Kiselva, I., Navrotsky, A., Belitsky, I.A. and Fursenko, B.A., 1996b. Thermochemistry of natural potassium sodium calcium leonhardite and its cation exchanged forms. American Mineralogist, 81: 668-675.

Kristmanndottir, H. and Tomasson, J., 1978. Zeolite zones in geothermal areas of Iceland. In: L.B. Sand and F.A. Mumpton (Editors), Natural Zeolites: Occurrence, Properties, Use. Pergamon, New York, pp. 277-284.

Liou, J.G., 1970. Synthesis and stability relations of wairakite, $CaAl_2SiO_4 \cdot 2H_2O$. Contributions to Mineralogy and Petrology, 27: 259-282.

Liou, J.G., 1971. Stilbite-laumontite equilibrium. Contributions to Mineralogy and Petrology, 31: 171-177.

McCulloh, T. H., Frizzell, V. A., Stewart, R. J., and Barnes, I., 1981. Precipitation of laumontite with quartz, thenardite, and gypsum at Sespe Hot Springs, Western Transverse Ranges, California. Clays and Clay Minerals, 29: 353-364.

Murphy, W.M., Pabalan, R.T., Prikryl, J.D. and Goulet, C.J., 1996. Reaction kinetics and thermodynamics of aqueous dissolution and growth of analcime and Na-clinoptilolite at 25 °C. American Journal of Science, 296: 128-186.

Nagy, K.L., Blum, A.E. and Lasaga, A.C., 1988. Dissolution and precipitation kinetics of kaolinite at 80°C and pH 3: The dependence on solution saturation state. American Journal of Science, 291: 649-686.

Pabalan, R.T., 1994. Thermodynamics of ion exchange between clinoptilolite and aqueous solutions of Na^+/K^+ and Na^+/Ca^{2+}. Geochimica et Cosmochimica Acta, 58: 4573-4590.

Petrovic, I. and Navrotsky, A., 1997. Thermochemistry of Na-faujasites with varying Si/Al ratios. Microporous Materials, 9: 1-12.

Sheppard, R.A. and Gude, A.J.I., 1969. Diagenesis of tuffs in the Barstow Formation, Mud Hills, San Bernardino, California, 597. U. S. Geological Survey Professional Paper, 38 pp. American Mineralogist, 67: 937-943.

Appendix A

EXPERIMENTAL METHODS

Solubility Experiments

Hydrothermal solubilities were measured in Ti-17 alloy or gold-plated, stainless steel autoclaves in rocking, dual-wound furnaces (Barnes, 1971; Wilkin and Barnes, 1997). Pressure was measured using a Heise Bourdon tube gauge accurate to within ± 0.1% of full scale. Temperatures were monitored and controlled using two premium quality, chromel-alumel thermocouples (Thermoelectric Company) inserted into the top and bottom of the autoclave. The thermocouples were calibrated by measurement of vapor pressure over pure water and with a Pt-resistance thermometer read with a Mueller bridge, DC power supply, and galvanometer. Solubility experiments were usually conducted at pressures along the liquid-vapor curve of the aqueous solutions.

Zeolite minerals have wide variations in water content. The absolute quantity of water in a particular zeolite can vary depending on temperature, humidity, and exchangeable cation composition (Boles, 1972). An advantage of aqueous solubility measurements on zeolites is that a constant state of maximum hydration can be maintained over the duration of an experiment.

This closed-system experimental design has been used extensively to investigate the thermochemical properties of minerals and aqueous species (e.g., Barnes, 1971; Crerar and Barnes, 1976; Giordano and Barnes, 1979; Bourcier and Barnes, 1987; Gammons and Barnes, 1989; Wilkin and Barnes, 1998). To ensure thermodynamic consistency, solubility measurements are made by approaching equilibrium conditions from both supersaturated and undersaturated states. Solution samples are withdrawn, pH measured, and analyses completed for total Si, Al, and Na, or other cations by ICP spectroscopy supplemented by ion chromatography as necessary.

Calculation of thermodynamic solubility products from the measured concentrations of Σ(Al), Σ(Si), and Σ(cations) in hydrothermal equilibrium with the zeolite requires knowing the dominant, stoichiometrically balanced dissolution reaction, a method of partitioning total analytical concentrations into the appropriate aqueous speciation, plus an ion-activity model to calculate activity coefficients for all aqueous species. Experimental solutions are speciated at temperature using selected thermodynamic constants (Wilkin and Barnes, 1997). Individual ion- activity coefficients are calculated using the 'B-dot' method of the extended Debye-Hückel equation with parameters from Helgeson and Kirkham (1974). For the neutral species, $Si(OH)_4$ and $Al(OH)_3$, activity coefficients are taken to be unity. Only monomeric species of Al and Si are assumed to be present in these low concentration solutions.

Below 100°C, experiments were made in 30- mL polyethylene bottles and their temperatures were maintained either at 50±2°C in a furnace or at room temperature. The

bottles are loaded with approximately 2 g of zeolite and about 20 mL of 5 m*m* sodium borate (or potassium borate) plus 7 m*m* HCl stock solution. The HCl is added to the solution to maintain a pH well below the first ionization constant of silicic acid. The suspensions are mixed by frequent (daily) inverting of the bottles several times. From these bottles, fluid samples are collected and filtered through 0.2 μm syringe filters, and then analyzed using the analytical methods described above. In these low-temperature experiments, zeolite solubilities could be approached only from undersaturated states.

Hydration Experiments

An important research accomplishment here has been the design and construction of a method to measure the hydration state of zeolites as a function of temperature and PH_2O. The system consists of a Ti-17 alloy reaction vessel (25.9 cm^3), a furnace, a high-precision pressure gauge (Heise), two calibrated K-type thermocouples (Thermoelectric Co.), and an HPLC pump (Scientific Systems, Inc.). *T* and *P* are measured for a reaction vessel containing precisely added quantities of clinoptilolite and water. At each *T* and *P*, the number of moles of water adsorbed by the zeolite is equal to the difference between the total amount of water in the system and the amount in the vapor phase calculated from the measured pressure, temperature, and vapor volume.

Measurements of *T* and *P* were made for experiments containing known amounts of clinoptilolite and water. At any *T* and *P* in the vapor-dominant region of pure H_2O, the number of moles of water adsorbed by clinoptilolite is equal to the difference between the total amount of water, $\Sigma(H_2O)$, inserted into the system and the amount of water in the vapor phase:

$$mH_2O_{cpt} = m_{\Sigma H2O} - mH_2O_{vapor} \qquad \text{(A1)}$$

The molar quantity of water vapor is calculated at any experimental temperature and pressure from the net internal volume (V) of the vessel and the *T*- and *P*-specific vapor volume, V_s, read from the steam tables by interpolating to the measured *P* and *T* by using:

$$mH_2O_{vapor} = [[V_{vessel} - (mass_{cpt} / \rho_{cpt})] / M_w V_s(P,T)] = PV / zRT \qquad \text{(A2)}$$

where z is the gas compressibility, *R* is the gas constant, *T* is the absolute temperature, *P* is the water vapor pressure, and M_w is the molecular weight of water. The stoichiometric coefficient of water in clinoptilolite (x) is then equal to the quotient of the moles of water in clinoptilolite divided by the molar quantity of clinoptilolite on an anhydrous basis. The experimental evaluation of x can then be used to determine reversible equilibrium constants and to derive an activity model for the clinoptilolite-water solid solution.

Kinetic Experiments

The experimental techniques used to measure congruent dissolution and precipitation rates have long been in routine use in our lab. These experiments were carried out using a dual-input, flow-through apparatus to measure reaction rates. Input solutions with

selected alkali and buffer concentrations are pumped from separate reservoirs by two high-pressure pumps through two nutrient bombs. The two output solutions are combined in a principal reaction vessel and out through a back-pressure regulator. The reaction vessel and nutrient feeder bombs are composed of either Ti-17 alloy or stainless steel, for, respectively, lower or higher pH experiments. This system design provides independent, adjustable flow rates and silica and aluminum concentrations into a reactor cell containing sized grains and quantities of minerals. Therefore, rates can be measured at constant saturation states, flow rates, pressures, and temperatures for runs up to months in duration if desired.

Dissolution or precipitation rates are derived from the concentration differences between the input and output solutions entering and leaving the reaction vessel. For example, the surface area-normalized dissolution rate, R (mole $m^{-2}sec^{-1}$), can be obtained from the expression:

$$R = \left(\frac{\partial moles(zeol.)}{\partial t}\right)_{P,T,A} = -\frac{q}{A\,\upsilon_i}(C_{i,out} - C_{i,in}) \qquad (A3)$$

where $C_{i,out}$ and $C_{i,in}$ are the concentrations of solutes, i, in the output and input solutions (moles/m^3), ν_i is the stoichiometric coefficient of i in the balanced dissolution reaction, A is the total surface area of the mineral (m^2), and ω is the fluid flux through the reaction vessel (m^3/sec). By convention the rate is positive for precipitation and negative for dissolution. Thus, reaction rates can be determined at any set of isothermal and isobaric conditions including the important saturation state (e.g., Nagy et al., 1991; Oelkers et al., 1994) which is easily described by:

$$\Delta G_r = \Delta G^\circ_r + RT \ln Q \qquad (A4)$$

where Q is the measured aqueous ion activity product for the mineral of interest. Note that the standard-state term, ΔG°_r, required for a complete kinetic description, is obtained directly from the solubility data described above. With the dual-input, flow-through system, ΔG_r can be precisely controlled so that reaction rates can be measured both near and far from equilibrium. In addition to sampling input and output fluid compositions, samples of solids may be extracted through a capillary tube that extends into the vessel. This allows solids to be analyzed for phase abundance, crystal size distribution, and mineral composition. As described below, this is an especially powerful method for studying rates and mechanisms of mineral transformation reactions in hydrothermal solutions.

Analytical Procedures

We used a variety of analytical techniques to monitor changes that occur in fluids and solids during the course of the proposed experiments.

1. The major element composition of fluids and solids were determined using ICP-emission spectroscopy plus ion chromatography, as needed. Room temperature pH was measured using a calibrated combination electrode and dedicated pH meter.

2. Solids were characterized before and after experiments by using powder X-ray diffraction techniques, optical microscopy, thermogravimetric techniques, Atomic Force Microscopy, Scanning Electron Microscopy, and Transmission Electron Microscopy, to quantify compositions, mineralogic content, and mineral textures.

3. Mineral compositions were checked by using electron micrprobe and wet chemical analyses.

4. The surface area of the initial and reacted solids were determined using state-of-the-art, B.E.T. adsorption methods.